Z. Physik A 288, 373–381 (1978)

Zeitschrift
für Physik A

Particle-Rotor Model for Doubly Odd Transitional Nuclei of the Tl-Region

A.J. Kreiner*
Fachbereich Physik der Technischen Universität München,
Garching, Fed. Rep. Germany

Received October 26, 1977, Revised Version July 31, 1978

A model has been investigated describing a situation in which two noninteracting high-j Nilsson-BCS quasiparticles move in the deformed field of an axially and reflection symmetric rotor. According to the positions of the j-shells with respect to the proton and neutron Fermi surfaces structures of different character emerge referred to as semi- and doubly-decoupled. In particular, strongly Coriolis-distorted bands recently reported in doubly odd Tl nuclei are discussed. Also $\tilde{\pi} h_{9/2}$ bands in neighbouring odd mass Tl isotopes are analysed on the same footing. It is shown that the pronounced odd even staggering of the transition energies can be understood as a specific quantal feature associated with the Coriolis interaction.

1. Introduction

Several rotational bands based on high-j unique-parity quasiparticle (qp) states ($\tilde{\pi} h_{9/2}$, $\tilde{\pi} h_{11/2}$, $\tilde{\nu} i_{13/2}$) have been reported in recent years in odd nuclei of the transitional region below the double shell closure at ^{208}Pb [1–7]. Hence, it is plausible to expect high spin structures, in the doubly odd nuclei built on intrinsic states just resulting from the vector addition of these qp excitations if the residual proton-neutron interaction does not obscures such a simple picture.

Thus, one may envisage two different cases in this part of the nuclidic chart. These two are $\tilde{\pi} h_{9/2} \otimes \tilde{\nu} i_{13/2}$ and $\tilde{\pi} h_{11/2} \otimes \tilde{\nu} i_{13/2}$. The first one actually appears to be realized in Tl [8, 9]. The second one is expected in more proton defficient nuclei like the Au isotopes where the $\tilde{\pi} h_{11/2}$ qp state is known to come nearer to the Fermi surface [8, 10].

The main aim of the present work is to show that, indeed, the simple picture referred to above is able to provide an explanation for all especial features found in the experiments.

* Present address: Departamento de Fisica, CNEA, Libertador 8250, Buenos Aires, Argentina

2. The Model

A brief account of the model will be given first (further details may be found in [8]). The Hamiltonian is:

$$H = A\mathbf{R}^2 + h_0^p + h_0^n \quad (A = h^2/(2\theta)). \tag{1}$$

$\mathbf{R}$ denotes the collective rotational angular momentum, only this degree of freedom is treated for the core. $h_0^{p(n)}$ is the Hamiltonian for the odd valence proton (neutron) describing the motion in the intrinsic coordinate system. It comprises a one-body operator for the average deformed field (a Nilsson Hamiltonian) and a two-body term which accounts for the pairing correlations treated in the BCS approximation. Since we are going to work in the strong coupling basic the usual substitution is made:

$$\mathbf{R} = \mathbf{I} - \mathbf{J} \quad (\mathbf{J} = \mathbf{j}_p + \mathbf{j}_n). \tag{2}$$

Thus, the rotational angular momentum becomes:

$$\mathbf{R}^2 = \mathbf{I}^2 - \mathbf{I}_3^2 - 2\mathbf{I}^{\perp} \cdot \mathbf{J} + \mathbf{j}_p^{\perp 2} + \mathbf{j}_n^{\perp 2} + 2\mathbf{j}_n^{\perp} \cdot \mathbf{j}_p^{\perp}. \tag{3}$$

The superscript $\perp$ denotes those parts of the vectors

0340-2193/78/0288/0373/$01.80

lying in a plane perpendicular to the symmetry axis.

In this contribution we shall discuss only cases in which both qp occupy high-j unique-parity states. The single j-shell approximation has been adopted which is known to be remarkably good for relatively small deformations ($|\beta|$ is certainly below 0.2 for the cases of actual interest). The configuration space for the intrinsic motion is thus spanned by allowing both protons and neutrons to move in two such subshells. The intrinsic states are product states of a quasineutron and a quasiproton which retain the quantum numbers of the Nilsson particles. All one-qp parts of the operator (1) were taken into account. No proton-neutron residual interaction has been considered. We believe that it is not necessary to include such a force in order to get agreement with the data. We shall discuss this problem later on. In order to get the right qp, the two superconducting equations were solved separately for protons and neutrons. Nilsson parameters were taken from [11]. Both pairing strenghts were adjusted so as to reproduce the gaps corresponding to the odd-even mass differences in this region. Thus, the model contains two parameters to be determined from the odd spectra, namely the inertial constant $\hbar^2/2\theta$ and the quadrupole deformation β. However, the customary prescription given by the Grodzins expression [12] for the moment of inertia ($\hbar^2/2\theta = 204\, A^{-7/3}\beta^{-2}$) has been adopted. The deformation is not extracted from the neighbouring even-even nuclei because of possible polarization effects and is regarded as the only adjustable quantity of the model. In practice, however, there is some uncertainty concerning single qp properties. It is difficult to get reliable single-particle energies and also the treatment of pairing is schematic. This leaves in turn, gap, Fermi levels and qp energies undetermined to some extent. In view of these facts we do not expect any nuclear model to give much more than a qualitative agreement without adjusting some parameter (within reasonable limits). It is just in the spirit of obtaining such a qualitative understanding that we want to study different phenomena and point out the main origins of them.

3. The "Semi decoupled" Case

3.1. General Discussion

This case will arise whenever one of the qp is in a decoupling situation and the other in a condition which is usually referred to as strongly coupled [13]. We want to illustrate this behaviour in the case of the $\tilde{\pi} h_{9/2} \otimes \tilde{\nu} i_{13/2}$ system because of the available data [8, 9].

Negative parity normal ($\Delta I = 1$) high-spin bands based on $I^\pi = 8^-$ isomers were found in ^{196,198}Tl respectively. In addition to the band head spin, two particular features displayed by the doubly odd cascades have to be explained by the model, namely: 1) the small initial transition energies (as compared to spacings in bands of related parentage in neighbouring nuclei, see below) and 2) the odd-even staggering in the excitation energies.

Once the Hamiltonian (1) is diagonalized we may evaluate several expectation values with the resulting wave functions. For this purpose it is necessary to define some quantities which will give us the appropriate insight into the structure of the states. Introducing a unit vector $\hat{\mathbf{e}}_I = \mathbf{I}/(I(I+1))^{1/2}$ pointing along the total angular momentum, the mean values $\langle \hat{\mathbf{e}}_I \cdot \mathbf{j}_n \rangle$ and $\langle \hat{\mathbf{e}}_I \cdot \mathbf{j}_p \rangle$ will thus measure the alignment of neutron and proton in this direction. More explicitly we have:

$$\langle \hat{\mathbf{e}}_I \cdot \mathbf{j}_n \rangle = (I(I+1))^{-1/2} \langle I_3 j_{n3} + 1/2 (I^+ j_n^- + I^- j_n^+) \rangle. \quad (4)$$

The relative orientation of the qp will be given by:

$$\cos(\mathbf{j}_n, \mathbf{j}_p) = \langle \mathbf{j}_n \cdot \mathbf{j}_p (j_n(j_n+1) j_p(j_p+1))^{-1/2} \rangle. \quad (5)$$

In addition, we shall study how the distributions over the corresponding magnetic substates of both qp evolve as the total spin of the system increases. This is important in order to characterize the orientations with respect to the symmetry axis. The occupation probability of a particular substate will be specified by:

$$|c^I_{\Omega_{p0}}|^2 = \sum_{K_\gtrless} |a^I_{K_\gtrless}(\Omega_n, \Omega_{p0})|^2. \quad (6)$$

($K_\gtrless = |\Omega_n \pm \Omega_p|$, $a^I_{K_\gtrless}$ being the expansion coefficients of the yrast wave function in the strong coupling basis [8].)

Some of these distributions are given in Figure 1 for the proton along with the $d^{9/2}_{9/2\Omega}(\pi/2)$ small Wigner matrices which correspond to a completely decoupled situation ($a^{9/2\dagger}_\alpha = \sum_\Omega d^{9/2}_{\alpha\Omega}(\pi/2)\, a^{9/2\dagger}_\Omega$ creates a particle in a state with projection α on the intrinsic 1-axis [14]). Actually the coupling scheme (if measured by these distributions) changes radically in going from the bandhead ($I = 8$) up to spin $I = 21$. At spin 8 the proton is mainly concentrated in the $\Omega_p = 9/2$ substate (which is the lowest qp state because we are dealing with a particle-like excitation in an oblate core), whereas for large (odd) spin states a nearly complete decoupling is reached.

The distributions for the neutron qp follow closely $d^{13/2}_{13/2\Omega}(\pi/2)$ (in accordance with the hole-like charac-

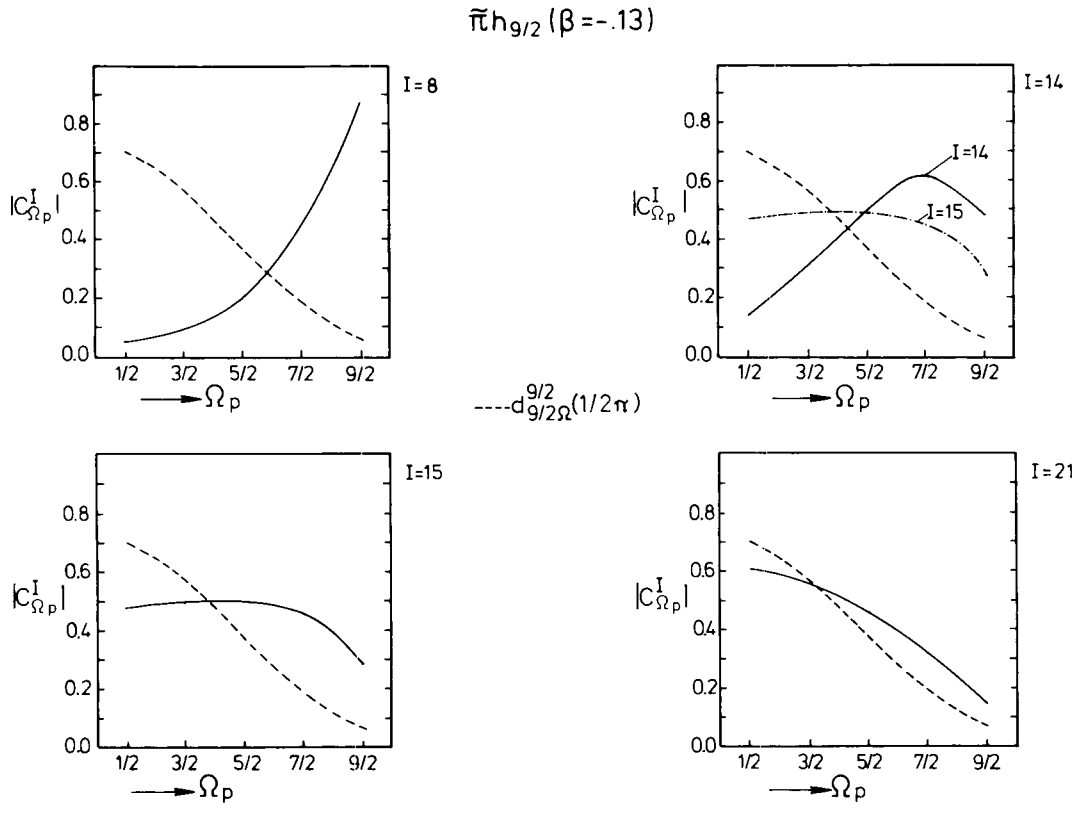

Fig. 1. Magnetic substate distributions for the $h_{9/2}$ proton. Parameters of the calculation are: $\beta = -0.13$ (Nilsson parameters from [11], $\hbar^2/2\,\theta = 204\,\beta^{-2}\,A^{-7/3}$, $\Delta_n \simeq 0.8$ MeV, $\Delta_p \simeq 0.9$ MeV. The distribution for $I = 15$ is also plotted (dotted and dashed) in the same frame as $I = 14$ in order to illustrate the staggering

Table 1. Different calculated expectation values for the $\tilde{\pi}h_{9/2} \otimes \tilde{\nu}i_{13/2}$ band (the calculation corresponds to the same parameter set as Fig. 1). (Angular momenta are given in units of $\hbar$)

I	R	$\langle \hat{\mathbf{e}}_I \cdot \mathbf{j}_n \rangle$	$\langle \hat{\mathbf{e}}_I \cdot \mathbf{j}_p \rangle$	$\cos(\mathbf{j}_n, \mathbf{j}_p)$	$\langle \lvert j_{n3} \rvert \rangle$	$\langle \lvert j_{p3} \rvert \rangle$
8	1.02	5.59	2.81	0.019	1.72	4.17
9	1.03	5.94	3.30	0.235	1.75	4.10
10	1.14	6.26	3.68	0.425	1.87	3.91
11	1.49	6.47	3.93	0.570	1.99	3.66
12	2.29	6.53	3.86	0.572	1.98	3.50
13	2.50	6.63	4.37	0.750	1.98	2.76
14	4.14	6.59	3.85	0.614	1.92	3.22
15	4.19	6.65	4.51	0.802	1.86	2.18
16	6.10	6.61	3.82	0.630	1.84	3.02
17	6.10	6.64	4.55	0.819	1.78	1.88
18	8.08	6.60	3.79	0.637	1.78	2.89
19	8.07	6.62	4.57	0.826	1.72	1.72
20	10.08	6.60	3.76	0.640	1.73	2.80
21	10.05	6.61	4.57	0.829	1.69	1.61

ter of this excitation) with minor deviations which will be discussed below. Incidentally, one notes that the band-head spin arises from the orthogonal coupling of both qp which, for the actual positions of the Fermi levels, represents the energetically most favourable configuration.

In order to complete the picture the expectation values defined above are given in Table 1. The collective angular momentum in the second column is defined as the physical root of the following quadratic equation:

$$\langle \mathbf{R}^2 \rangle = R(R+1). \tag{7}$$

R is seen to be smallest for the $I = 8$–11 multiplet. For these states the projection $\langle \hat{\mathbf{e}}_I \cdot \mathbf{j}_n \rangle$ and also $\langle \lvert j_{n3} \rvert \rangle$ (the mean of the absolute value of j_{n3}) increases. On the other side $\langle \hat{\mathbf{e}}_I \cdot \mathbf{j}_p \rangle$ also grows but $\langle \lvert j_{p3} \rvert \rangle$ becomes smaller indicating that $\mathbf{j}_p$ inclines towards the equatorial plane. In this form the largest part of the spin is obtained from the intrinsic motion. It is easier, from the standpoint of the required energy, to obtain angular momentum by changing the orientation of the qp in the weakly deformed oblate field instead of increase the core-rotation (as should occur if the adiabatic condition held). These facts offer an explanation for point I).

From here on the system must start to add collective spin (recall $(\mathbf{9/2 + 13/2})_{\max} = \mathbf{11}$). Unfavoured (unf) (even spin) and favoured (fav) (odd spin) states have practically the same core spin expectation value

(and also similar R-value distributions as will be shown later). In going from one given even spin state to the following odd one it is again energetically more convenient for the system to gain the single unit of angular momentum by tilting the proton in the direction of **I**. The next even member of the band is built by adding two units of rotational angular momentum and $\mathbf{j}_p$ is released away in the direction of the symmetry axis. In this connection it is interesting to point out that the amplitudes $|c^I_{\Omega_p}|$ in the unf states compare asymptotically with $d^{9/2}_{7/2\Omega}(\pi/2)$.

From $I=11$ on the neutron remains attached to **I** and $\langle|j_{n3}|\rangle$ decreases slowly. All vectors involved in the description of the system become progressively aligned with the rotation axis. The strong staggering in the transition energies reflects itself in the large signature [15] dependent variation of the quantities belonging to the proton (the signature is defined as the quantum number $(-1)^I$).

Up to this point all of our arguments made in order to provide a qualitative understanding of the staggering phenomenon were based on the least-energy principle. As a matter of fact, however, the appearance of such a feature is of specific quantal nature. The special form of the yrast wave function is, of course, under the given curcumstances and for a proper quantum mechanical treatment of our problem a consequence of the abovementioned principle, but it is also true that the generalized signature dependent effect will not show up in a classical system. From such a point of view it should be expected that a monotonic increase (with I) of the Coriolis force would also cause a monotonic increase in $\langle\hat{\mathbf{e}}_I\cdot\mathbf{j}_p\rangle$.

The analytical origin of the phenomenon under discussion is encountered in the signature dependent part of some non-diagonal Coriolis matrix elements. A large number of matrix elements (or parts of them) change sign alternatively with I acting coherently in one or the other direction. Essential to this process are the states with $K=0$ and 1, all signature dependent parts of the matrix elements are proportional to $\delta_{K',-K+1}$, i.e. those connecting the "direct" and $\mathscr{R}$-reflected [15] parts of the wave functions.

3.2. Comparison with the Data and Odd Tl Nuclei

We have collected in Table 2 data concerning the gsb of ^{194,196}Hg [16, 17] (which represent the relevant cores for the Tl nuclei under discussion), the recently reported $\tilde{\pi}h_{9/2}$ bands in odd mass Tl isotopes [6, 7] and the available information on the negative parity bands in doubly odd ^{196,198}Tl [8, 9]. Some comments are necessary about the doubly odd data. The parallelism between the two $\tilde{\pi}h_{9/2}\otimes\tilde{\nu}i_{13/2}$ bands in ^{198}Tl and ^{196}Tl (starting from the 122.2 and 108.6 keV γ-rays respectively) is remarkable and therefore we are forced to admit that the transition in ^{198}Tl corresponding to the 61.5 keV γ-ray in ^{196}Tl was not detected (in fact, in order to achieve a good time resolution the constant-fraction-trigger discrimination levels were set above the Tl X-rays in that experiment, see [8]). In addition, it cannot be concluded from our measurements if there are other unobserved cascade transitions below the 61.5 keV γ-ray. Due to the large internal conversion the de-excitation will no longer proceed through γ-emission below a certain transition energy. The X-γ coincidence experiment [9] just set an upper limit of about 35 keV for the eventually unobserved transitions. However, as may be seen in the last column of Table 2, the theory predicts in a very definite manner

Table 2. Ground state bands of ^{194,196}Hg [16, 17], $\tilde{\pi}h_{9/2}$ bands in ^{195,197}Tl [6, 7] and negative parity bands in ^{196,198}Tl [8, 9]. Also theoretical results are shown (see text)

I^π_{e-e}	I^π_o	I^π_{o-o}	^{194}Hg ΔE_I[a] (exp)	^{195}Tl ΔE_I (exp)	^{196}Tl ΔE_I (exp)	^{196}Hg ΔE_I (exp)	^{197}Tl ΔE_I (exp)	^{197}Tl ΔE_I ($\tilde{\pi}h_{9/2}\otimes{}^{196}$Hg)	^{197}Tl ΔE_I (rig. rotor)	^{198}Tl ΔE_I (exp)	^{198}Tl ΔE_I (theor.)
0^+	$9/2^-$	8^-									
		9^-			< 35					?	18
		10^-			61.5					?	67
		11^-			108.6					122.2	140
2^+	$11/2^-$	12^-	428.4	394.2	271.4	426.1	387.6	373	374	259.0	231
	$13/2^-$	13^-		313.2	236.4		307.9	286	318	246.0	242
4^+	$15/2^-$	14^-	636.8	428.6	396.9	635.3	416.1	448	741	401.5	531
	$17/2^-$	15^-		305.8	266.7		298.9	270	312	296.7	271
6^+	$19/2^-$	16^-	734.7	545.7	447.8	723.5	407.8	440	1240	488.6	918

[a] Transition energies are given in keV. $\Delta E_I=E_I-E_{I-2}$ for $e-e$ nuclei and $\Delta E_I=E_I-E_{I-1}$ for odd (o and $o-o$) nuclei

a single additional transition; otherwise the calculated staggering would be opposite in phase to the measured one (the parameters of the calculation are the same of Fig. 1). At the same time Table 2 shows that the staggering behaviour is already present in the $\tilde{\pi} h_{9/2}$ bands of neighbouring odd Tl isotopes and appears to be of similar magnitude (especially for states with $I \geqq 15/2$ and 14 respectively). This fact strongly suggests the same origin in both cases. It is also seen (if the above hypothesis holds) that the especial features present in the experimental spectra are qualitatively well reproduced by the model calculations, the main failure being the overestimation of the fav$(I) \rightarrow$ unf$(I+1)$ spacings. Nevertheless, this fact is exclusively related to the inappropriate representation of the core spectrum by a rigid rotor, as will be shown in following paragraphs. In doing so we shall take a way around the odd mass Tl isotopes.

Much theoretical work has been done on odd Tl isotopes. The first investigations were made with the particle-plus-rotor model (PRM), assuming an axially symmetric rigid rotator (sometimes also including terms of higher order in $\mathbf{R}^2$) [18]. After that, the model was improved by the inclusion of triaxial shapes [19–21] which increases the agreement mainly due to the better representation of the compressed rotational spectrum in the core nucleus as compared to the axially symmetric case. In the next step allowance was made for the softness of the core in a VMI [22] fashion [23] and finally the complete Bohr Hamiltonian has been solved for some especial potential energy surfaces [24]. The increasing complexity (and the increasing number of parameters) has probably made it difficult to isolate the causes giving origin to some specific features. We have, therefore, returned to the starting point and reinvestigated the PRM in its most simple form in order to discuss the staggering. The clarification of this point seems important to us, because it has been repeatedly suggested [19, 21, 25] that the staggering (and in particular the approach of the $11/2_1^-$ and $13/2_1^-$ states, which is nothing but the first step of the staggering) is a feature connected especifically with the γ degree of freedom while this phenomenon already appears in our doubly odd calculations without breaking away from axial symmetry. In column 10 of Table 2 the results of a calculation are shown where the PRM-Hamiltonian (rigid, axially symmetric) for the $\tilde{\pi} h_{9/2}$ system has been diagonalized. Again here the fav$(I+1) \rightarrow$ unf(I) spacing are well reproduced but the other ones are also greatly overestimated. Table 3 displays some expectation values showing a very similar behaviour as in the doubly odd case. (There is a difference for the band head state due to the fact that no neutron is present. Here $\mathbf{R} = \mathbf{I} - \mathbf{j}_p \simeq \mathbf{0}$ and therefore the large value of $\langle \hat{\mathbf{e}}_I \cdot \mathbf{j}_p \rangle$.) We see (Table 3) that the phenomenon which becomes apparent in the staggering of the transition energies also appears in the signature dependent variation of all expectation values (the signature will be taken here as $(-1)^{I+1/2}$). The primary analytical origin of the effect is the diagonal matrix element $(\hbar^2/2\theta)\delta_{K,1/2}(-1)^{I+1/2} a_p(I+1/2)$ (a_p being the decoupling parameter). It depresses the fav states $(9/2, 13/2, \ldots)$ and raises the unf ones $(11/2, 15/2, \ldots)$. Of course, the other nondiagonal (but signature independent) Coriolis matrix elements are needed in order to couple the $\Omega_p = 1/2$ state to the other members of the j-shell multiplet. The low energy of this $\Omega_p = 1/2$ orbital (in the fav states) allows the admixture of additional low Ω_p subtates, leading finally to the decoupling. (In fact, an explanation pointing in the same direction but in the framework of perturbation theory has been discussed in [1].) The effect is really important for high j orbits where the decoupling parameter takes eventually its maximal value. Without this matrix element, decoupled bands would not exist (this term is as large as $\simeq 3.2$ MeV already for the band heads of $\tilde{\nu} i_{13/2}$ decoupled bands in odd mercurys) even though $\mathbf{j}$ will be aligned to some (increasing) extent in all members of the cascade, what indeed occurs in a classical system. Here the rotational yrast spectrum tends to separate in two parts of opposite signature. This specific quantal feature is intimately connected with the reflection symmetry of the deformation. From this point of view the only difference between nuclei showing decoupled bands and bands of the normal type ($\Delta I = 1$) is the energetic placement of the decoupled state in the fermion (qp) spectrum. Results of Tables 2 and 3 correspond to a qp spectrum obtained at $\beta = -0.115$ and $\Delta_p \simeq 0.9$ MeV.

We intend to demonstrate now that the inability of the model to describe the fav$(I) \rightarrow$ unf$(I+1)$ transitions has certainly to be ascribed to the assumption of rigidity for the core. The quasirotational behaviour of these gsb is far from following the $I(I+1)$ law.

Table 3. Some average values for the $h_{9/2}$ band (rigid rotor calculation)

I^a	R	$\langle \hat{\mathbf{e}}_I \cdot \mathbf{j}_p \rangle$	$(\langle j_{p3}^2 \rangle)^{1/2}$	$\langle h_0^p \rangle$ (keV)
9/2	0.78	4.74	4.06	1236
11/2	2.07	4.44	3.85	1274
13/2	2.31	4.66	3.06	1505
15/2	4.07	4.19	3.46	1372
17/2	4.10	4.68	2.45	1663
19/2	6.05	4.05	3.22	1433
21/2	6.05	4.66	2.15	1732

[a] Angular momenta in units of $\hbar$

However, instead of proposing a particular description for them, the following procedure is adopted. The collective part of the Hamiltonian is supposed to exhibit a general dependence on $\mathbf{R}^2$ (thus implying axial symmetry). Moreover, the eigenvalues are taken from the experimental spectrum ($H_c(\mathbf{R}^2)|RM\rangle = E_R|RM\rangle$; $E_R = E_R^{\exp}$) and the states of the gsb are chosen to be structureless axially symmetric Wigner functions. A similar method has been explored in [26], with a somewhat different point of view, yielding analogous results as ours. The Hamiltonian to be diagonalized is:

$$H = H_c(\mathbf{R}^2) + h_o^p. \tag{8}$$

In order to handle the first right hand side term the strong coupling wave function is expanded in a basis of eigenfunctions of the core spin:

$$|IKM\rangle = \sum (2(2R+1)/(2I+1))^{1/2} \cdot (jKR0|IK)|(jR)IM\rangle. \tag{9}$$

(The summation is restricted to even R values satisfying $|I-j| \leqq R \leqq I+j$.) $|(jR)IM\rangle$ represents the vector coupling of the qp(j) in the laboratory system and the rotor state. The matrix element of $H_c(\mathbf{R}^2)$ becomes:

$$\langle IKM|H_c(\mathbf{R}^2)|IK'M\rangle = 2(-1)^{K+K'+1} \sum_{R_{\text{even}}} (2R+1) \cdot E_R \begin{pmatrix} j & R & I \\ K & 0 & -K \end{pmatrix} \begin{pmatrix} j & R & I \\ K' & 0 & -K' \end{pmatrix}. \tag{10}$$

The results of this calculation are also given in Table 2 (column 9) labeled as $\tilde{\pi} h_{9/2} \otimes {}^{196}\text{Hg}$ and the agreement is satisfactory. Parameters employed here are the same as those of col. 10 with the only exception being the proton Fermi level (λ_p) which was lowered $\simeq 400$ keV with respect to the value of the rigid rotor calculation (which corresponds to the solution of the number equation) in order to compensate for the somewhat different Coriolis effects present when one couples to the experimental core states. This quantity has revealed itself as an important one, because it determines the position of the $\Omega_p = 1/2$ and other low Ω_p states (A lowering of λ_p relative to the $h_{9/2}$ shell will eventually supress the staggering in the first step).

In order to look somewhat closer into the outcome of such a calculation we show in Figure 2 the resulting distributions in R-space along with the unperturbed

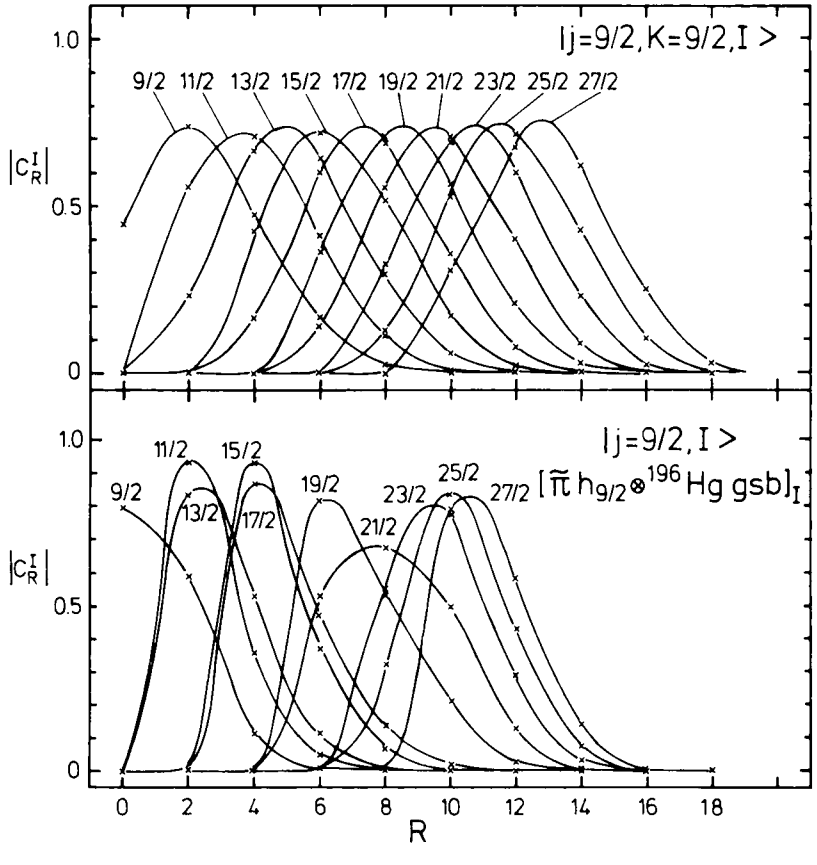

Fig. 2. Expansion amplitudes of the strong coupling states in terms of core eigenfunctions (upper part) are compared with the actual states of the $\tilde{\pi} h_{9/2}$ band as emerging from the $\tilde{\pi} h_{9/2} \otimes {}^{196}\text{Hg}$ calculation

strong coupled ($|j=9/2,\ K=9/2,\ I\rangle$) states. The transformation relating the expansions of the final wave function in both representations is given by:

$$c_R^I=(2(2R+1))^{1/2}\sum_K c_K^I(-1)^{K+j}\begin{pmatrix} j & R & I \\ K & 0 & -K\end{pmatrix}. \qquad (11)$$

The distributions over R for the actual states are radically different from those for the unperturbed ones. They are much narrower and shifted to lower values. Corresponding fav and unf states have similar amplitudes (the fav-ones being broader). We believe the procedure to be reliable for spin values up to $I=\frac{15}{2},\frac{17}{2}$ which are mainly related to core states with $I\leqq 4$. The $I=\frac{19}{2},\ \frac{21}{2}$ pair represents a limiting case going parallel with the appearance of the discontinuity in the gsb of ^{196}Hg [16, 17]. This is indeed reflected in the change of character of the distributions of these states (especially for $I=21/2$). Above $I=6$ the description in terms of rotating BCS vacuum core states is no longer acceptable, the two-qp structure [16] has to be taken into account explicitly.

It is seen that the qualitative pictures emerging from both calculations ($\tilde{\pi}h_{9/2}\otimes$ rig. rot. and $\tilde{\pi}h_{9/2}\otimes{}^{196}$Hg) are the same. What we would like to stress once more is that the only essential difference concerns the better representation of the core, the fav$(I+1)\rightarrow$unf(I) spacings being mainly determined by the qp spectrum, are equally well reproduced in both cases.

Let us make a final remark on non-yrast states. Usually, the existence of a second $13/2^-$ state has been taken as a strong indication of triaxiality in odd Tl isotopes [21]. On the other hand, however, the γ-deformation of $\simeq 40°$ tend to underestimate the $13/2_1^-\rightarrow 11/2_1^-$ spacing [21, 24]. It might be that the 2_2^+ state (head of the quasi-γ band) in even Hg plays an important role in the description of the $13/2_2^-$ but this does not necessarily imply the existence of a static γ-deformed field governing the dynamics of the yrast band.

3.3. *The Problem of the Residual Interaction*

As has been extensively discussed in the preceding sections we are very confident that the basic mechanism responsible for the odd-even staggering is provided by the Coriolis force. It is also clear that any other signature dependence will contribute to the effect if it has the same phase as the latter one. However, it has been pointed out recently [27] that the origin of the staggering in ^{198}Tl is a residual interaction between proton and neutron taken in the model calculations as a modified surface delta force. In addition to the results presented so far, there is a further argument which disfavours such an explanation. It will be shown that a residual interaction with similar characteristics as found in a nearlying region of the nuclidic chart gives in fact a signature dependent contribution which has the opposite phase as needed to explain the staggering. In [28] the experimental splitting of the $\pi h_{9/2}\otimes\nu i_{13/2}^{-1}$ multiplet obtained in ^{208}Bi is reported (see Table 4, column 3). The particle hole (p-h) interaction behaves just opposite to the particle-particle (p-p) one which is obtained in the last column applying the Pandya transformation [29]. The angle between the two spins is obtained semiclassically according to:

$$\cos(\mathbf{j}_n,\mathbf{j}_p)=(J(J+1)-j_p(j_p+1)$$
$$-j_n(j_n+1))(4j_p(j_p+1)j_n(j_n+1))^{-1/2}.$$

The smooth interpolation of the p-p behaviour is typical for a short range interaction between non-identical particles, being most effective for the smallest and largest spins where the spatial overlap is maximal. Also, the behaviour of the interaction of the $h_{9/2}$ proton with the entire $i_{13/2}$ shell minus one particle is expected (here the maximal overlap is achieved for the orthogonal coupling). On the other hand, the (fav) odd spin states of the cascade correspond to larger values of the intrinsic angular momentum compared to the unf ones (see Table 1). This means that the odd spins will be pushed up in energy as far as the expectation value of the interaction is involved (calculated with the unsymmetrized part of the wave functions). It must be said, however, that the interaction itself has also signature dependent matrix elements. But in this case only $K=0$ components of the states may contribute (for a scalar interaction), therefore we do not expect the main effect to be obscured.

Table 4. Energy splitting of the $\pi h_{9/2}\otimes\nu i_{13/2}^{-1}$ multiplet in ^{208}Bi (from [28])

J^π	$\cos(\mathbf{j}_n,\mathbf{j}_p)$	$E_J^{\text{p-h}}$(MeV)	$E_J^{\text{p-p}}$(MeV)
2^-		1.353	−1.563
3^-		0.377	0.727
4^-		0.296	0.367
5^-		0.160	−0.312
6^-		0.173	−0.147
7^-		0.173	−0.229
8^-	−0.017	0.116	−0.080
9^-	0.241	0.224	−0.279
10^-	0.530	0.023	−0.052
11^-	0.839	0.886	−0.678

This argument is considered to be valid because every acceptable short range attractive interaction must show similar features, especially in the case of high spin orbitals with spatially well localized wave functions.

4. The $\tilde{\pi} h_{11/2} \otimes \tilde{\nu} i_{13/2}$ Doubly Decoupled Case

This structure has been already discussed [8, 10] and will be just briefly reviewed. In the present case both qp have predominantly hole character. Hence, due to the fact that we are considering the coupling to an oblate core the small Ω_n and Ω_p components lie nearest to the corresponding Fermi surfaces. The yrast band is now a decoupled sequence based on a 12^- state. The features of this band are radically different to those found in the semidecoupled situation. The resulting structure is of $\Delta I = 2$ type, resembling the even-even core and has states connected by collective $E2$ transitions. In fact, such 12^- isomers were known for some time in ^{196,198}Au [30] and more information would be desirable in order to further test these ideas.

5. Conclusion

A very simple and transparent model like the PRM is shown to be able to provide a qualitative understanding of all particularities found in recent experiments. Mainly the semidecoupled $\tilde{\pi} h_{9/2} \otimes \tilde{\nu} i_{13/2}$ structure has been discussed. Actually a similar behaviour is expected whenever one of the two qp has a decoupled state which lies energetically high. One may say, that in this case the doubly decoupled band is situated higher than the first unfavoured one. It is possible to imagine all intermediate cases between the two extreme situations discussed. The actual behaviour will depend on the specific position of the Fermi level with respect to the relevant shell and also on the value of the deformation.

Perhaps more interesting are the conclusions connected with the understanding of the staggering feature. Normally the "strongly coupled" situation is characterized by stating that the Coriolis force is not able to overcome the interaction with the deformed field. However, the picture emerging here cannot be completely understood in just those terms. The similarity between decoupled and $\Delta I = 1$ structures is probably greater than usually believed regarding the appropriate quantum numbers needed for their description and becomes apparent when a decomposition in R-space is performed. (The statement is of course restricted to odd bands of high-j provenience.) Coriolis effects are very large in both cases, the particular character being just determined by the position in the qp spectrum of the rotation-aligned state. As a matter of fact, as soon as the energetic splitting of the intrinsic configuration space tends to disappear (measured in units of $\hbar^2/2\theta$) the corresponding fav and unf states of opposite signature degenerate.

In axially deformed even-even systems the spins of the gsb are limited to even values by the reflection symmetry of the shape. In odd (and doubly odd) nuclei where such a restriction does not exist, states of both signatures are allowed. The Coriolis force acting in these reflection symmetric systems gives rise to the special features discussed.

The author wants to acknowledge sincerely the hospitality of Prof. H. Morinaga and all members of the E17 Institute at the Technical University Munich and the support by the DAAD (Deutscher Akademischer Austauschdienst). The extremely efficient technical assistance of Miss U. Heim is also gratefully acknowledged.

References

1. Newton, J.O., Cirilov, S.D., Stephens, F.S., Diamond, R.M.: Nucl. Phys. A **148**, 593 (1970)
2. Newton, J.O., Stephens, F.S., Diamond, R.M.: Nucl. Phys. A **236**, 225 (1974)
3. Proetel, D., Benson Jr., D., Gizon, A., Gizon, J., Maier, M.R., Diamond, R.M., Stephens, F.S.: Nucl. Phys. A **226**, 237 (1974)
4. Tjom, P.O., Maier, M.R., Benson, D. Jr., Stephens, F.S., Diamond, R.M.: Nucl. Phys. A **231**, 397 (1974)
5. Gono, Y., Lieder, R.M., Müller-Veggian, M., Neskakis, A., Mayer-Böricke, C.: Phys. Rev. Lett. **37**, 1123 (1976)
6. Lieder, R.M.: in: Proc. Int. Symp. on Collectivity of Medium and Heavy Nuclei, Tokyo, 1976, Y. Shida (ed.), p. 459
7. Lieder, R.M., Neskakis, A., Müller-Veggian, M., Gono, Y., Mayer-Böricke, C., Beshai, S., Fransson, K., Linden, C.G., Lindblad, Th.: to be published
8. Kreiner, A.J., Fenzl, M., Lunardi, S., Mariscotti, M.A.: J. Nucl. Phys. A **282**, 243 (1977)
9. Kreiner, A.J., Fenzl, M., Kutschera, W.: submitted to Nucl. Phys.
10. Toki, H., Yadav, H.L., Faessler, A.: Phys. Lett. **66** B, 310 (1977)
11. Davidson, J.P.: Collective Models of the Nucleus. New York: Academic Press 1968
12. Grodzins, L.: Phys. Lett. **2**, 88 (1962)
13. Stephens, F.S.: Rev. Mod. Phys. **47**, 43 (1975) and references therein
14. Stephens, F.S., Diamond, R.M., Nilsson, S.G.: Phys. Lett. **44** B, 429 (1973)
15. Bohr, A., Mottelson, B.R.: Nuclear Structure, Vol. 2. New York: Benjamin 1975
16. Proetel, D., Diamond, R.M., Stephens, F.S.: Nucl. Phys. A **231**, 301 (1974)

17. Lieder, R.M., Beuscher, H., Davidson, W.F., Neskakis, A., Mayer-Boricke, C.: Nucl. Phys. A **248**, 317 (1975)
18. Stephens, F.S., Diamond, R.M., Benson, D., Jr., Maier, M.R.: Phys. Rev. C **7**, 2163 (1973)
19. Meyer-ter-Vehn, J., Stephens, F.S., Diamond, R.M.: Phys. Rev. Lett. **24**, 1383 (1974)
20. Meyer-ter-Vehn, J.: Nucl. Phys. A **249**, 11 (1975)
21. Meyer-ter-Vehn, J.: Nucl. Phys. A **249**, 141 (1975)
22. Mariscotti, M.A.J., Goldhaber, G.S., Buck, B.: Phys. Rev. **178**, 1864 (1969)
23. Toki, H., Faessler, A.: Nucl. Phys. A **253**, 231 (1975)
24. Leander, G.: Nucl. Phys. A **273**, 286 (1976)
25. Slocombe, M.G., Newton, J.O., Dracoulis, G.D.: Nucl. Phys. A **275**, 166 (1977)
26. Tanaka, Y., Sheline, R.K.: Nucl. Phys. A **276**, 101 (1977)
27. Toki, H., Yadav, H.L., Faessler, A.: Phys. Lett. **71** B, 1 (1977)
28. Schiffer, J.P., True, W.W.: Rev. Mod. Phys. **48**, 191 (1976)
29. Shalit, A. de, Feshbach, H.: Theoretical Nuclear Physics, Vol. 1. New York: Wiley & Sons 1974
30. Nuclear level schemes $A=45$ through $A=257$ form Nucl. Data Sheets, ed. Nucl. Data Group. New York: Academic Press 1973

Dr. A.J. Kreiner
Departamento de Fisica
Comisión Nacional de Energia Atómica
Libertador 8250
RA-1429 Buenos Aires
Argentina